BASIC SCIENCE

Nanomedicine: Nanotechnology, Biology, and Medicine
24 (2020) 102147

Original Article

nanomedjournal.com

Mycophenolate co-administration with quercetin *via* lipid-polymer hybrid nanoparticles for enhanced breast cancer management

Gopal Patel, PhD[a,c,1], Neeraj Singh Thakur, PhD[a,1], Varun Kushwah, PhD[b], Mahesh D Patil, PhD[d], Shivraj Hariram Nile, PhD[c], Sanyog Jain, PhD[b], Guoyin Kai, PhD[c,*], Uttam Chand Banerjee, PhD[a,*]

[a]*Department of Pharmaceutical Technology (Biotechnology), National Institute of Pharmaceutical Education and Research, S.A.S. Nagar, Punjab, India*
[b]*Centre for Pharmaceutical Nanotechnology, Department of Pharmaceutics, National Institute of Pharmaceutical Education and Research, S.A.S. Nagar, Punjab, India*
[c]*Laboratory of Medicinal Plant Biotechnology, College of Pharmacy, Zhejiang Chinese Medical University, Hangzhou, Zhejiang, PR China*
[d]*Department of Systems Biotechnology, Konkuk University, Seoul, Republic of Korea*

Revised 27 November 2019

Abstract

Mycophenolic acid (MPA) has promising anticancer properties; however, it has limited clinical applications *in vivo* due to hydrophobic nature, high first-pass metabolism, lack of targeting, *etc*. These associated problems could be addressed by developing a suitable delivery vehicle, inhibiting the first-pass metabolism and additive/synergistic pharmacodynamic effect. Thus, MPA loaded highly stable lipid polymer hybrid nanoparticles (LPNs) were developed and investigated with the combination of quercetin (QC), a CYP 450 inhibitor *cum* anticancer. LPNs of MPA and QC (size; 136 ± 12 and 176 ± 35 nm, respectively) demonstrated higher cellular uptake and cytotoxicity of combination therapy (MPA-LPN + QC-LPN) compared to individual congeners in MCF-7 cells. *In vivo* pharmacokinetics demonstrated 2.17 fold higher $T_{1/2}$ value and significantly higher pharmacodynamic activity in case of combination therapy compared to free MPA. In nutshell, the combinatory therapeutic regimen of MPA and QC could be a promising approach in improved breast cancer management.

Key words: Mycophenolic acid; Quercetin; Anticancer; Hybrid nanoparticles; Co-administration

Mycophenolic acid (MPA) is an immunosuppressant drug mainly produced *by Penicillium brevicompactum, P. roqueforti, P. stoloniferum* and other fungal species.[1–6] MPA is mainly used as an immunosuppressant, arthritis and other autoimmune disorder,[7–10] *via* selectively inhibiting enzyme inosine monophosphate dehydrogenase (IMPDH) resulting in reduced *de novo* synthesis of lymphocytes.[3,11,12] In-addition, the IMPDH was also reported to play a vital role in cancer,[7,13] highlighting the importance of MPA as an anticancer agent.[7–9,14] Moreover, Zheng et al reported that MPA exhibited potent agonist activity against peroxisome proliferator-activated receptor gamma (PPARγ) which has a central role in the inhibition of proliferation of cancer cells.[8] Furthermore, inhibition of cancer cell proliferation, metastasis inhibition and induction of apoptosis by MPA were also reported in some other studies.[15–17] In spite of promising anticancer potential, the clinical application of the MPA is severely hindered owing to lower oral bioavailability and dose-dependent off targeted side effects.[18,19] Moreover, MPA is primarily metabolized *via* cytochrome P450 into inactive metabolite 7-O-glucuronide (MPAG) resulting in reduced bioavailability and pharmacodynamic efficacy. Shirali et al and Look et al developed PLGA and liposome nanoparticles with improved *in vivo* bioavailability and efficacy of MPA against skin transplantation and systemic lupus erythematosus (SLE), respectively.[20,21] Hwang et al reported biomedical applications, including drug delivery, of MPA loaded iron oxide nanoparticles.[22] However, very few reports are available indicating amelioration in anticancer efficacy of MPA. There is no report available with a function of improved bioavailability and reduced metabolism. In line with this, the development of MPA lipid polymer hybrid nanoparticles (LPN) and co-delivery of quercetin (a known CYP 450 inhibitor) could be the best way to improve the MPA's bioavailability and anticancer efficacy. LPNs have been widely used to deliver bioactive molecules for the treatment of various

Acknowledgments: Not applicable.

Funding: This research did not receive any specific grant from funding agencies in the public, commercial, or not-for-profit sectors.

Conflict of Interest: All authors declare that he/she has no conflict of interest.

*Corresponding authors.

E-mail addresses: kaiguoyin@163.com (G. Kai), ucbanerjee@niper.ac.in (U.C. Banerjee).

[1] These authors contributed equaly.

https://doi.org/10.1016/j.nano.2019.102147
1549-9634/

diseases including cancer because of the following advantages: favorable stability in biological environments, decrease drug doses, sustained drug release ability and reduce toxicity. LPNs are reported as advanced delivery vehicle over the conventional metallic or polymeric nanoparticles due to three distinct functional components: 1) a hydrophobic biodegradable polymeric core (PLGA) to encapsulate poorly water-soluble drugs with higher loading yield and sustained release of encapsulated drug; 2) an inner lipid monolayer enveloping the hydrophobic core, the main function of which is to confer biocompatibility and to promote drug retention inside the polymeric core; and 3) a hydrophilic polymer stealth layer (PEG) outside the lipid shell which can augment the nanoparticles stability and body circulation lifetime.[23–25]

Quercetin (QC), a flavonoid, is reported to have diverse pharmacodynamic actions such as antioxidant, anti-inflammatory, antiaging, anticancer, hepatoprotective and cardioprotective, *etc.*[26,27] In addition, QC demonstrated to have cytochrome P450 (CYP450) enzyme inhibitory properties which could play a vital role in the rapid metabolism of MPA.[28,29] Thus, the co-administration of QC with MPA may augment the therapeutic efficacy of MPA by increasing the bioavailability of MPA and synergistic cytotoxic effects. Nano preparations of these drugs further increase the efficacy by increasing the bioavailability, targeted delivery and higher tumor accumulation (through increased vascular permeability).

Present work described the preparation of MPA encapsulated lipid polymer hybrid nanoparticles (MPA-LPN) and quercetin encapsulated lipid polymer hybrid nanoparticles (QC-LPN) and further extensively characterized (*in vitro* and *in vivo*) for efficient breast cancer management. The co-administration of MPA-LPN and QC-LPN has demonstrated higher bioavailability, reduced off-target toxicity, higher tumor accumulation, and higher anticancer activity. As demonstrated by the breast cancer management, co-administration of MPA-QC through nano formulations may be further utilized for other cancer treatment and/or to improve solid organ transplant outcomes with minimized drug toxicities. To the best of our knowledge, this is the first-ever attempt to improve the bioavailability and efficacy of MPA through co-administration with QC for the treatment of breast cancer disease.

Methods

Preparation and characterization of nanoparticles

The reported nanoprecipitation method was used for the preparation of LPNs.[30,31] Briefly, the aqueous phase was prepared by dissolving Pluronic® F-68 (7.5 mg), soya lecithin (2.25 mg) and 1,2-distearoyl-sn-glycero-3-phosphoethanolamine-N-[amino(poly-ethylene glycol)] (0.225 mg) in 4% ethanol-aqueous solution. To prepare the organic phase, poly (D, L-lactide-co-glycolide) acid (7.5 mg) and MPA (0.75 mg) were dissolved in 1 mL acetone. For better dispersion of the lipid molecule, the aqueous phase was heated to 60 °C temperature for some time. Afterward, the organic phase (dropwise) 1 mL/min was added into aqueous phase in bath sonicator at fixed sonication then the reaction mixture was stirred for 1.5 h at 300 rpm. Subsequently, the organic phase was evaporated by rotavapor from reaction mixture then acquired nanosuspension was lyophilized and characterized using various techniques which were furnished in the supplementary information (section S2.1).[10,32–35] Simultaneously, QC loaded LPNs were also prepared individually using the same procedure as above. The procedure to evaluate the encapsulation efficiency, drug release, and stability has been furnished in the supporting information (sections S2.2-S2.4).

In vitro cell culture experiments

Cells

MCF-7 (ATCC, USA) human breast cancer cell lines have been used to perform the *in vitro* cell culture experiments. ATCC protocols were followed for the media preparation and culture conditions. For cell uptake and apoptosis analysis, 50,000 cells/well were seeded in 6-well culture plate whenever. However, 10,000 cells/well in 6 well plates (Costars, Corning Inc., NY, USA) were used to determine the cell viability of MCF-7 cells through MTT assay.[36,37]

In vitro cytotoxicity assay

The cytotoxic effect of various samples was evaluated in MCF-7 cell lines using the MTT assay. The MCF-7 cell were seeded to 96 well plate and incubated overnight as per the ATCC protocol. After attachment of cells new media containing free MPA, free QC, free MPA + free QC (1:1 molar ratio) and various LPNs (MPA-LPN, QC-LPN, and MPA-PLN + QC-LPN) in separate wells were added at concentrations of 10, 20, 40 and 60 μg/mL each. Viable cells of mitochondria reduce tetrazolium component (MTT) into an insoluble formazan. These formazan crystals were dissolved DMSO and optical density (OD) of the samples was measured at 540 nm.[37] OD has a linear relationship with the number of viable cells and the cell viability was evaluated by Eq. (1):

$$\text{Relative cell viability} = (\text{Sample Absorbance}/\text{Control Absorbance}) \times 100 \quad (1)$$

Cell uptake

For cell uptake analysis, 50,000 cells/well in a 6-well plate were incubated overnight for the cell attachment. After attachment, the cells were exposed to free Coumarin-6 (C-6) and C-6 loaded LPNs (equivalent to 1 μg/mL C-6) for 2 h. Afterward, the medium was eliminated and cells were rinsed (twice) using PBS (pH 7). The cells were fixed with 2.5% (v/v) glutaraldehyde (Sigma, USA), washed, and observed under the confocal laser scanning microscope (CLSM, Olympus FV1000).[37]

Annexin V apoptosis assay

Further to confirm the cytotoxic effect, apoptosis assay was performed in the MCF-7 cell line using annexin V binding based standard phosphatidylserine externalization. MCF-7 cell lines with a fresh medium having different preparations (free MPA, free QC, free MPA + free QC, MPA-LPN, QC-LPN, and MPA-LPN + QC-LPN) were incubated for 6 h at 37 °C temperature and 200 rpm. After that, cells were rinsed three time with HBSS and stained with annexin V-Cy3.18 conjugate (AnnCy3) and 6-carboxyfluorescein diacetate (6-CFDA) as per the standard protocol of manufacturers (annexin V-Cy3™ apoptosis detection kit, Sigma, USA). Subsequently, 6-CFDA and AnnCy3 dyes in the cell were observed using CLSM under green and red channels, respectively. The red and green fluorescence in stained

cells reflected live and necrotic cells, respectively; however, cells showing both red and green fluorescence were considered as apoptotic. Further, a quantitative estimation of apoptosis was also carried out in the form of an apoptotic index in which a ratio of red and green fluorescent cells was calculated.[37]

Inosine-5′-monophosphate dehydrogenase (IMPDH) assay

The IMPDH inhibitory activity of various test samples was determined using the IMPDH assay kit (Biomedical Research Service & Clinical Application, USA). Mechanistically, iodonitrotetrazolium (INT) reduced into INT-formazan through an NADH-coupled reaction, and absorbance was recorded at 492 nm. IMPDH activity was measured in the MCF-7 cell line by treating with DMSO (control), 10 μM free MPA, and 10 μM MPA-LPN after 24 h of incubation.[38]

In vivo pharmacokinetics

Animals, dosing, collection and quantification

In vivo pharmacokinetics of MPA and QC NPs were evaluated in female SD rats of 200-250 g weight, provided by the central animal facility, NIPER, India. Animals approved by the Institutional Animals Ethics Committee (IAEC1717), NIPER, SAS Nagar, were maintained and treated following the guideline of the National Institutes of Health. Before the experiments, familiarization of animals was carried out at 25 ± 2 °C temperature and 50-60% relative humidity under the natural environment (light/dark) for one week. Animals were kept on fasting overnight before the start of the experiments and were allowed water *ad libitum*. After that, animals were arbitrarily divided into 7 groups (5 animals in each group). A different group of animals received i.p. free MPA (25 mg/kg), free QC suspension (25 mg/kg), combination of free MPA and free QC (25 mg/kg MPA and 25 mg/kg QC), MPA nanoparticles, QC nanoparticles and combination of MPA and QC nanoparticles (25 mg/kg equivalent to MPA and QC). At different time intervals (0.5, 1, 2, 6, 12, 24, and 48 h) blood samples (approximately 0.3 mL) were collected from the tail vein into heparinized microcentrifuge tubes. After each sampling, 1 mL dextrose–normal saline was administered orally to partially compensate the electrolyte level and central compartment volume. The blood samples were centrifuged at 10,000 rpm for 10 min and 4 °C temperature for the separation of plasma and later stored at −80 °C for further analysis.[9,14,30,39,40] MPA and QC quantification in the collected plasma samples was carried out using quantitative HPLC[37,41]; detailed procedures of quantification have been furnished in the supplementary information (Section S3).

Pharmacokinetic data analysis

For this study kinetic data of plasma concentration *vs* time were investigated by one compartmental model using Kinetica™-software (Thermo Fisher Scientific, USA). Essential pharmacokinetic conditions such as area under the curve $(AUC)^{0-\infty}$, maximum plasma concentration (C_{max}) and time to reach half of the maximum plasma concentration ($T_{1/2}$) were determined.[42,43]

In vivo antitumor efficacy and tissue distribution

DMBA (7, 12-dimethyl[a] benzanthracene) induced breast tumor-bearing female SD rats were employed for evaluating the antitumor efficacy of free MPA, free QC, free MPA + free QC, QC-LPN, MPA-LPN, and MPA-LPN + QC-LPN. Breast tumors were induced by oral administration of DMBA solution in soybean oil (45 mg/kg) to female SD rats (200-230 g) at weekly intervals for three consecutive weeks. Measurable tumor size was observed after 10 weeks of the last dose of DMBA. Tumor-bearing animals were separated and randomly divided into seven treatment groups. The first group of animals received the saline solution and served as the control, while other groups of animals received free MPA, free QC, free MPA + free QC, MPA-LPN, QC-LPN and MPA-LPN + QC-LPN. The administered dose of the MPA and QC was 25 mg/kg in all samples. During the study, tumor width (W) and length (L) were recorded with an electronic digital caliper and tumor size was calculated using the formula ($L \times W^2/2$). All the formulations were i.p. administered in a repeated dose (once in 3 days) and tumor growth was monitored up to 30 days. After the 30th day of treatments, the rats were sacrificed and the tumors were detached and washed with cold PBS. The size of tumors was noted. In sacrificed rats, the amounts of MPA and QC in various organs were also determined.[9,37,43,44]

Table 1
The characteristic features of prepared MPA-LPN and QC-LPN.

Parameters	MPA-LPN	QC-LPN
Average zeta size (nm)	136.11 ± 12.4	176 ± 34.65
Average zeta potential (mV)	−32.12 ± 3.14	−38.5 ± 3.65
PDI	0.017 ± 0.002	0.185 ± 0.018
TEM size (nm)	125	163
Shape	Spherical	Spherical

Toxicity study

To study the *in vivo* toxicity of developed nanoparticles different blood biochemical marker concentrations were performed. Blood specimens of sacrificed were taken in the heparin-containing (40 IU/mL of blood) microcentrifuge tubes, by cardiac puncture. For the separation of plasma, sample tubes were centrifuged for 10 min at 10,000 rpm. The spectrophotometric method was used by respective diagnostic kit protocol (Accurex biochemical Pvt. Ltd., India) to determine the concentration of various toxicity markers [*e.g.* blood urea nitrogen (BUN), creatinine, aspartate aminotransferase (AST), and alanine aminotransferase (ALT)].[37,43,45]

Statistical analysis

The data were stated as the mean of three separate experiments with error bars shown as a standard deviation. One-way analysis of variance was carried out using GraphPad Prism for all data sets and $P < .05$ was reflected statistically significant.

Results

Preparation of nanoparticles and characterization

The lipid-polymer hybrid nanoparticle of MPA and QC was successfully prepared. DLS analysis suggested the critical quality attributes such as particle size of prepared MPA-LPN and QC-LPN which was found to be 136.11 ± 12.4 and 176 ± 34.65 nm, respectively, while the respective zeta potentials were recorded as −32.12 ± 3.14 and −38.5 ± 3.65 mV (Table 1). The size distribution curves of MPA-LPN and QC-LPN were shown in Figure 1, *C* and *D*, respectively. Polydispersity indices (PDIs) of MPA-LPN

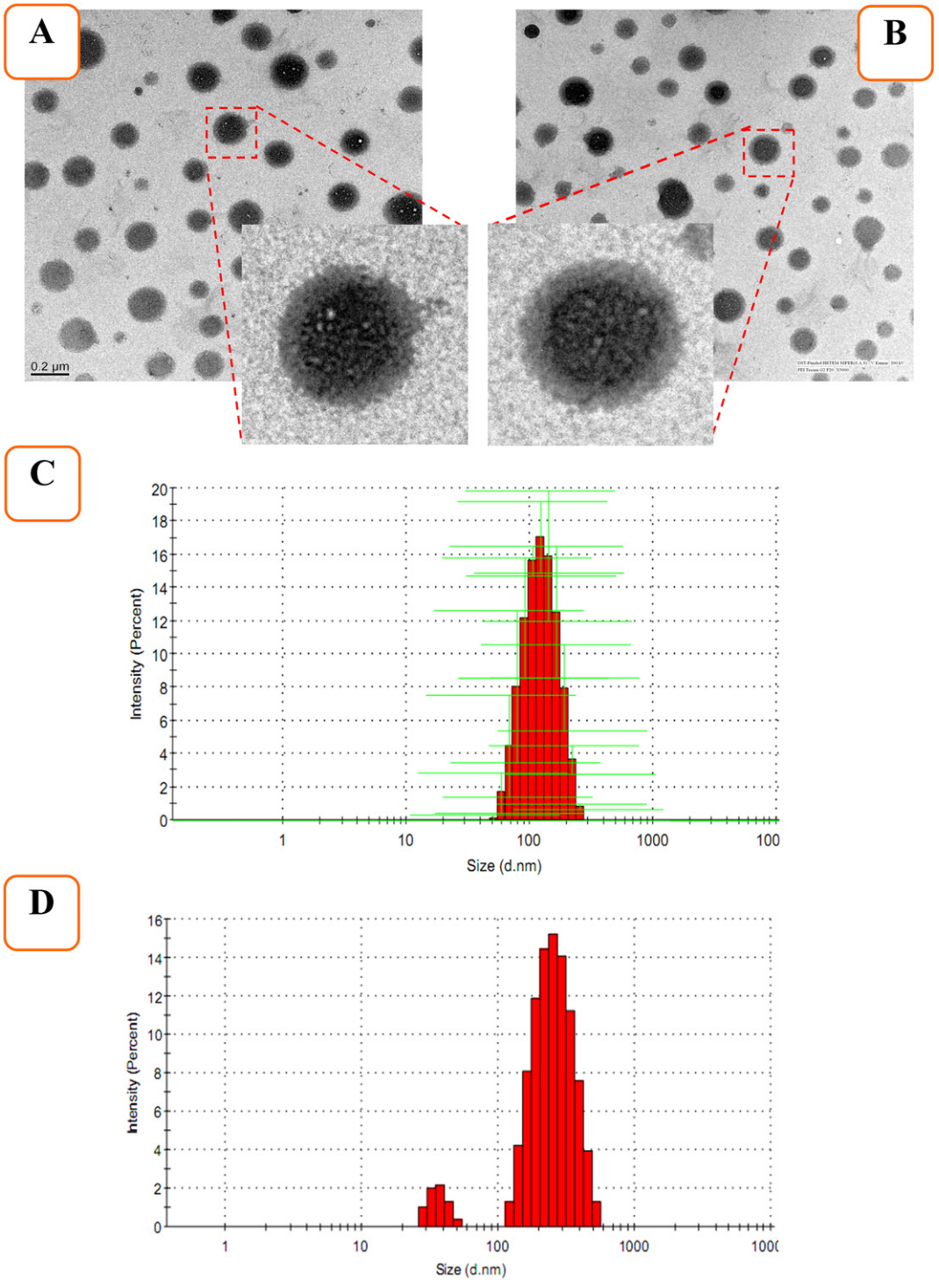

Figure 1. TEM images of prepared **(A)** MPA-LPN, **(B)** QC-LPN both on the scale of 200 nm; particle size distribution (**C**) MPA-LPN, (**D**) QC-LPN.

and QC-LPN were 0.017 ± 0.002 and 0.185 ± 0.018, respectively, further confirming the development of monodisperse and narrow size distribution of the nanoparticles. In addition, TEM demonstrated the formation of spherical and smooth-surfaced MPA-LPN and QC-LPN with the particle size 125 and 164 nm, respectively (Figure 1, *A* and *B*).

The FTIR analysis of free QC, free MPA, bare LPNs, QC-LPNs and MPA-LPNs was shown in Figure 2, *A* and these observations indicated that there was no significant intermolecular interaction that occurred in free MPA, free QC, bare LPN, MPA-LPN, and QC-LPN. However, the encapsulation of the drugs into the LPNs was determined by quantification studies using HPLC. The XRD

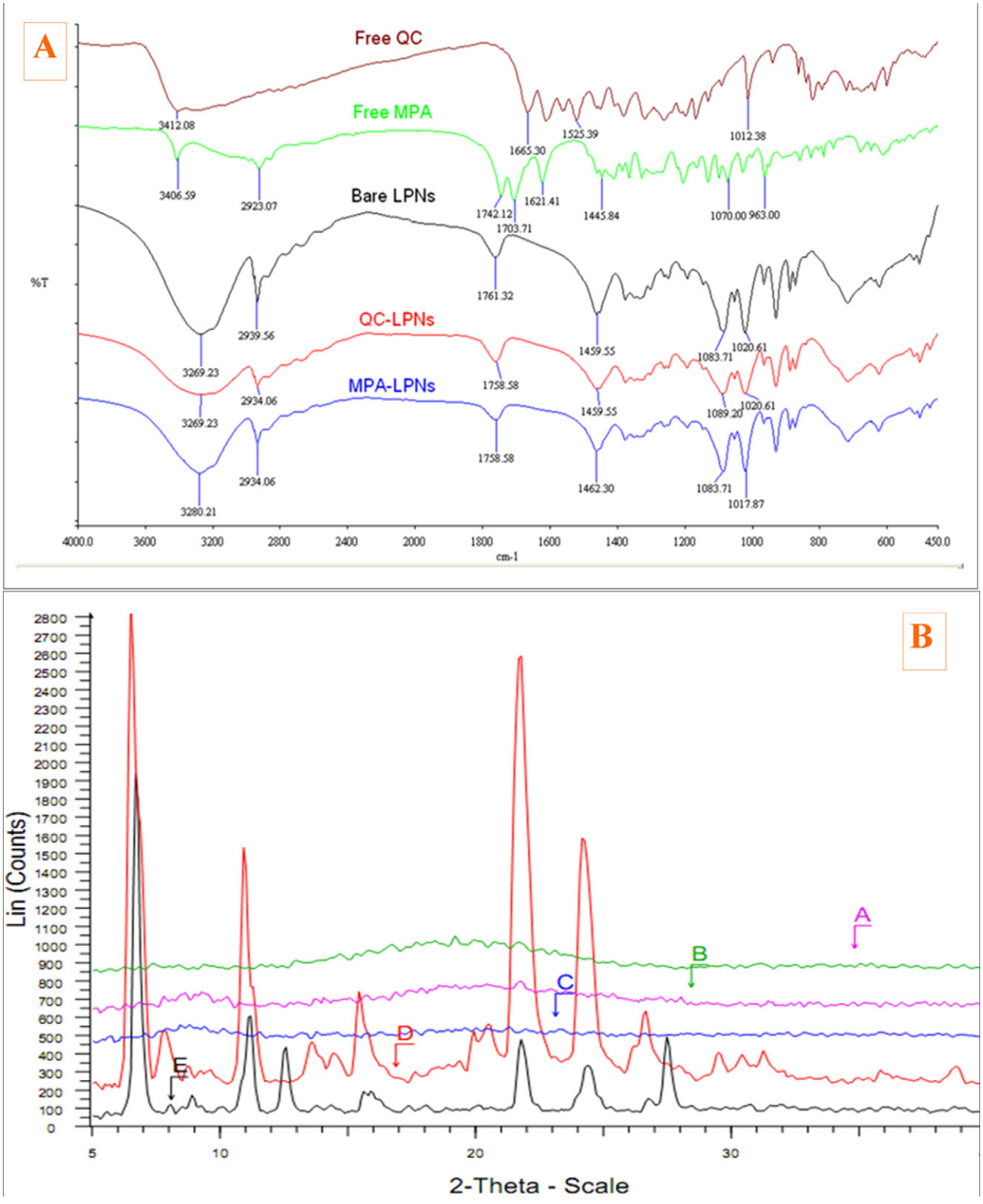

Figure 2. **(A)** FTIR pattern of free QC, free MPA, bare LPNs, QC-LPN and MPA-LPN. **(B)** XRD pattern of **A:** MPA-LPN, **B:** QC-LPN, **C:** LPN without the drug, **D:** free QC and **E:** free MPA.

analysis of free QC, free MPA, bare LPNs, QC-LPNs and MPA-LPNs was also carried out (Figure 2, *B*). The characteristic peaks of free QC and free MPA confirmed their crystalline structure in the respective PXRD spectrum, whereas no peaks were observed in the case of QC-LPN and MPA-LPN confirmed the presence of MPA and QC in their molecular form into the LPNs.

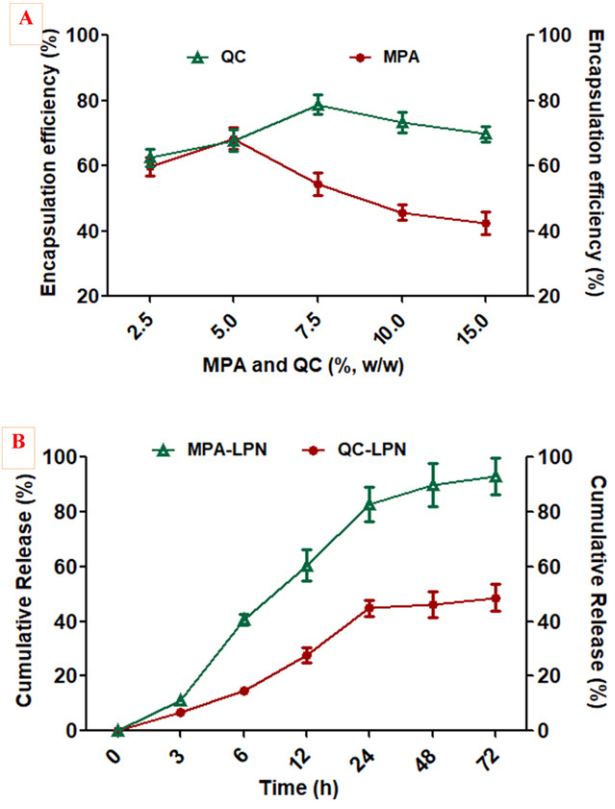

Figure 3. **(A)** Effect of MPA concentration on encapsulation efficiency (%) in the case of MPA-LPN. **(B)** Drug release profile of MPA-LPN and QC-LPN,

Table 2
Freeze drying of MPA-LPN using various cryoprotectants at a fixed concentration (5%, w/w).

Cryoprotectants	Without freeze drying	With freeze drying
Mannitol		
Size (nm)	136.11 ± 12.4	143.0 ± 8.2
Ri		1.05 ± 0.04
RS		[a]
Sucrose		
Size (nm)	136.11 ± 12.4	153.5 ± 13.9
Ri		1.42 ± 0.09
RS		[b]
Trehalose		
Size (nm)	136.11 ± 12.4	152.2 ± 8.6
Ri		1.12 ± 0.07
RS		[a]

Ri, redispersibility index; RS, reconstitution score. Values are presented as mean ± SD (n = 3).
[a] Redispersible within 20 s with mere mixing.
[b] Reconstitution requires high shear vortexing for 2 min.

Encapsulation efficiency and in vitro drug release of nanoparticles

Encapsulation of a drug into the nanoparticle plays a very important role in further clinical applications. MPA and QC concentrations were optimized to optimum particle size and PDI and higher drug encapsulation efficiency (% E.E) of nanoparticles. It has been confirmed from Figure 3, *A* that minimum encapsulation occurred at 15 (%, w/w) and maximum at 5 (%, w/w) of MPA respective to PLGA weight. On the other hand, the maximum encapsulation efficiency (78.23%) of QC was found at 7.5 (%, w/w) of QC with respect to the PLGA weight.

The release of MPA and QC from the prepared LPN is shown in Figure 3, *B*. The releasing rate of MPA was initially high up to 12 h in which around 60% of the drug came out followed by a sustained release up to 48 h with the release of a total 90% MPA. Quercetin release from QC-LPN (Figure 3, *B*) was also initially high up to 24 h during which 45% of the drug was released; however, the release rate became very slow after 24 h.

Table 3
Freeze drying of MPA-LPN using mannitol at different concentrations.

Cryoprotectant	Without freeze drying	With freeze drying			
		Concentration (%, w/w)			
Mannitol		0	2.5	5	10
Size (nm)	136.11 ± 12.4	ND	151.3 ± 10.4	147.0 ± 8.2	141.7 ± 8.6
Ri	-	ND	1.09 ± 0.06	1.05 ± 0.04	1.03 ± 0.05
RS	-	[c]	[b]	[a]	[a]

Ri, redispersibility index; RS, reconstitution score; ND, not determined due to incomplete redispersion of cake. Values are presented as mean ± SD (n = 3).
[a] Redispersible within 20 s with mere mixing.
[b] Redispersible within 1 min.
[c] Reconstitution requires high shear vortexing for 2 min, but the cake was not completely redispersed.

Table 4A
Characterization of MPA-LPN after six months of accelerated stability studies.

Parameters	Initial	Final
Particle size (nm)	147.0 ± 8.2	153.08 ± 20.14
PDI	0.017 ± 0.003	0.021 ± 0.032
Zeta potential (mV)	−27.12 ± 2.32	−23.8 ± 5.18
Ease of reconstitution	[a]	[a]
Physical appearance	Intact fluffy cake	Intact fluffy cake

Values are presented as mean ± SD (n = 6).
[a] Redispersible within 20 s with mere mixing.

Table 4B
Characterization of QC-LPN after six months of accelerated stability studies.

Parameters	Initial	Final
Particle size (nm)	182 ± 22.4	174.04 ± 21.61
PDI	0.172 ± 0.014	0.154 ± 0.029
Zeta potential (mV)	−34.2 ± 3.21	−31.6 ± 2.8
Ease of reconstitution	[a]	[a]
Physical appearance	Intact fluffy cake	Intact fluffy cake

Values are presented as mean ± SD (n = 6).
[a] Redispersible within 20 s with mere mixing.

Freeze-drying of LPNs

Different properties *viz.* reconstitution nature, size ratio and physical appearance of freeze-dried LPNs are shown in

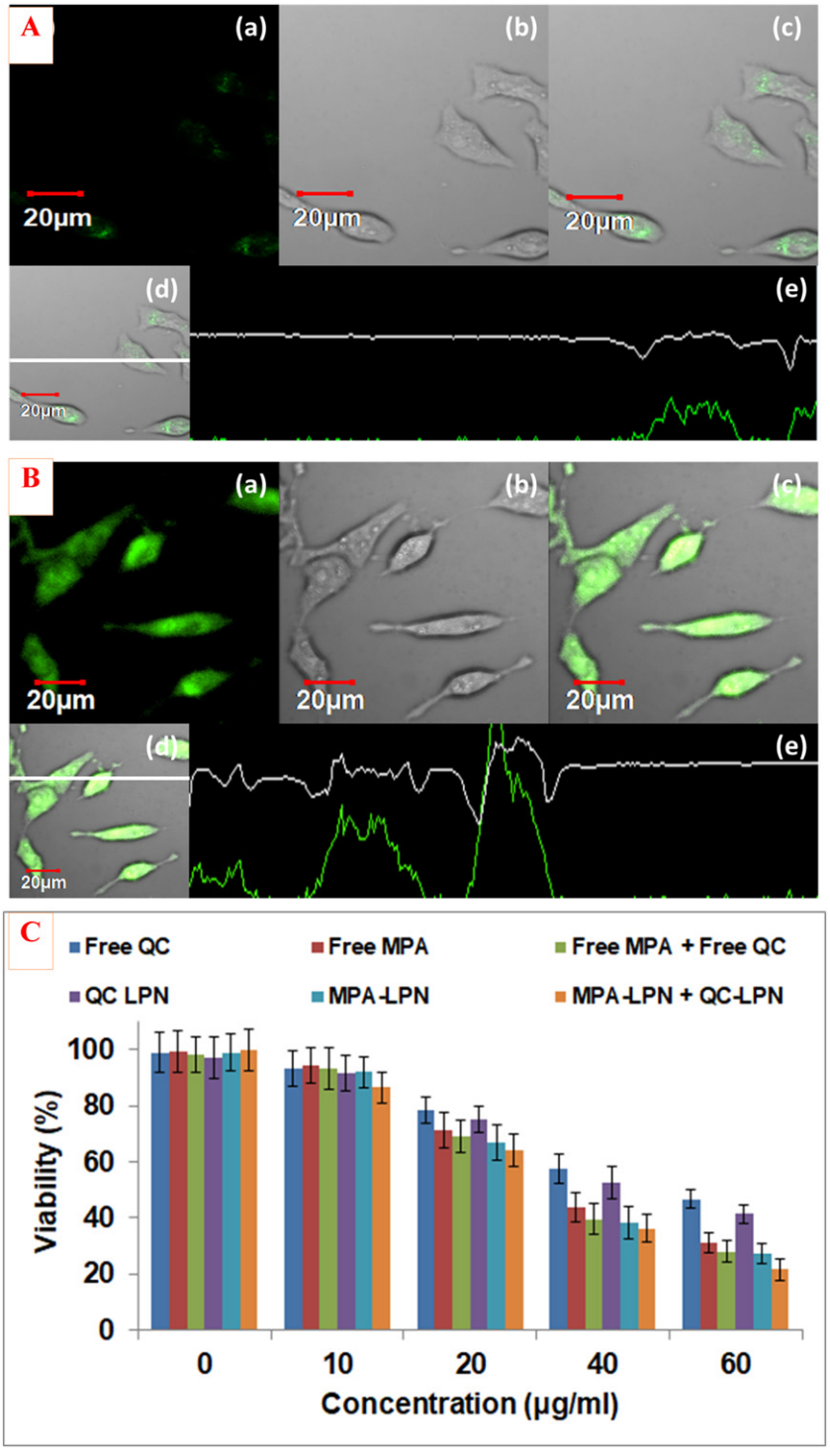

Figure 4. Uptake of **(A)** free C-6 and **(B)** C6-LPN by MCF-7 cells. **(a)** Green fluorescence of C-6. **(b)** Corresponding DIC images. **(c)** Overlay of **a** and **b**, and **(d** and **e)** vertical and horizontal line series analysis long the white line of image **c**. **(C)** Cell cytotoxicity of free QC, free MPA, combination of free MPA + free QC, QC-LPN, MPA-LPN and combination of MPA-LPN + QC-LPN after 24 h. Each data point represented as mean ± SD (n = 4).

Tables 2 and 3. Mannitol and trehalose (5%, w/w) resulted in the formation of intact, voluminous, fluffy and easy to redisperse cake, while the cake was not integral in the case of sucrose as cryoprotectant. A significant increase in particle size was observed following the freeze-drying without any cryoprotectants while the difference was insignificant when various cryoprotectants were used in different concentrations. Based on the appearance, the redispersibility index and reconstitution score, mannitol (5%, w/w) was selected as an optimized one.

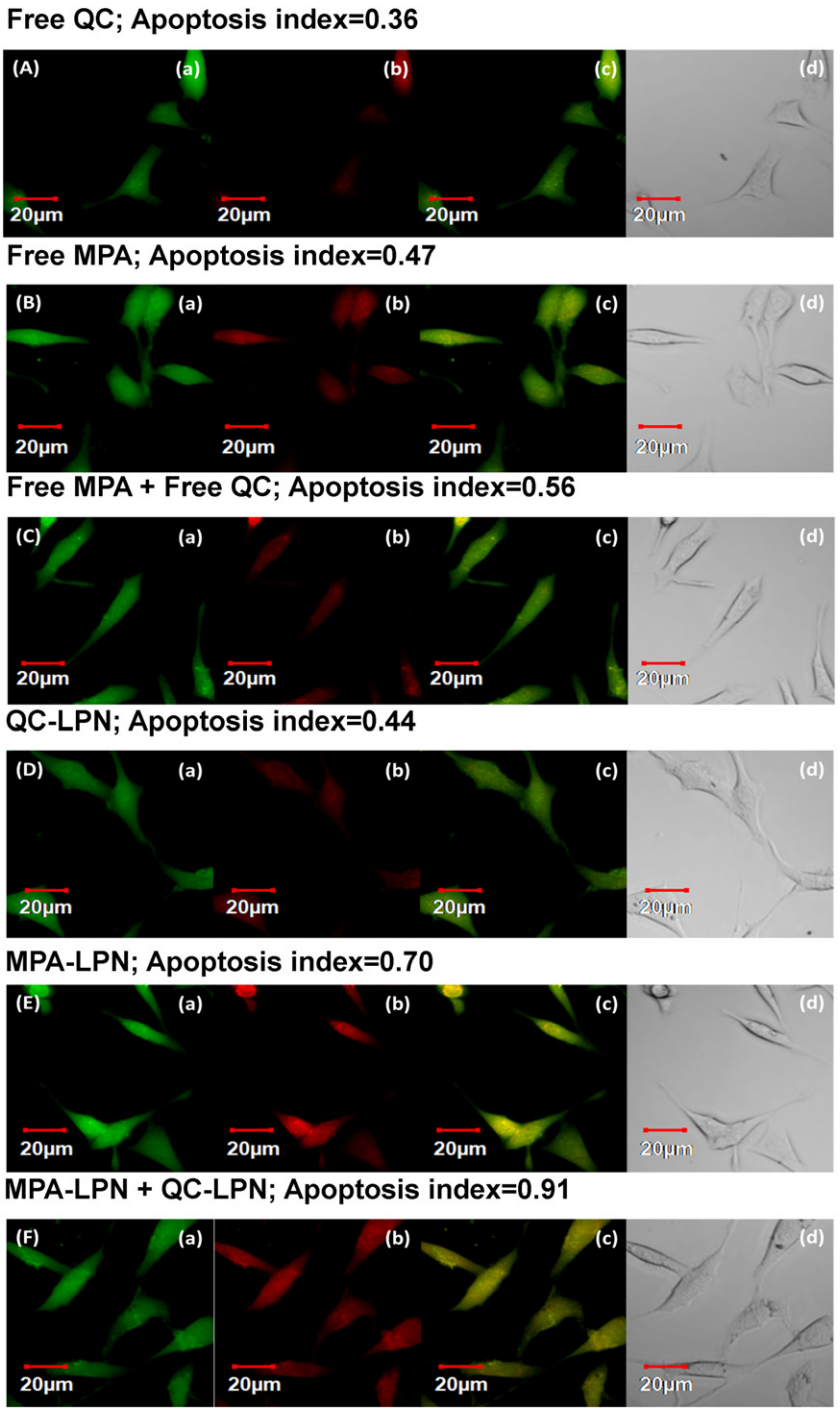

Figure 5. Apoptosis assay of free QC, free MPA, combination of free MPA + free QC, QC-LPN, MPA-LPN and combination of MPA-LPN + QC-LPN against MCF-7 cell line.

Accelerated stability of LPNs

Accelerated stability studies of MPA-LPN and QC-LPN were carried out for 6 months at 25 ± 2 °C and RH 60 ± 5% as per the ICH guidelines. Freeze-dried LPN of MPA and QC showed no change in terms of shrinkage of cake or any other change in physical appearance. Insignificant ($P > 0.05$) increases in the zeta potential, particle size, and PDI of prepared nanoparticles were found after the 6 months of the testing period (Tables 4A & 4B).

In vitro cell culture experiments

In vitro cellular uptake of LPNs and cytotoxicity assay

Qualitative cell uptake analysis was carried out in MCF-7 cells with C6 loaded NPs and free C-6 (1 μg/mL, 2 h).

Compared to free C6 (Figure 4, *A*), a significantly higher fluorescence was observed inside the cells after 2 h of incubation with C6 loaded nanoparticles (Figure 4, *B*). *In vitro* cell cytotoxicities of free MPA, free QC, free MPA + QC, MPA-LPN, QC-LPN, and MPA-LPN + QC-LPN were evaluated on MCF-7 cell lines. Figure 4, *C* revealed that cell cytotoxicity was more in nanoparticle preparations as compared to free drugs and their combination against MCF-7 cell lines. Furthermore, combination treatment of nanoparticles (MPA-LPN + QC-LPN) has shown significantly higher cytotoxic effect in MCF-7 cell line compared to individual nano preparation (MPA-LPN and QC-LPN).

Annexin V apoptosis assay

Apoptosis assay was used for the further confirmation of *in vitro* cytotoxicity results in MCF-7 cell line. The Annexin-V assay was performed and a quantitative analysis of apoptosis cells was carried out using CLSM by calculating the apoptotic index. The apoptotic indices of free MPA, free QC, Free MPA + free QC, MPA-LPN, QC-LPN, and MPA-LPN + QC-LPN were estimated and mentioned in Figure 5. Apoptosis indices of LPNs (MPA-LPN; 0.70 and QC-LPN; 0.44) were found to be higher compared to respective free drugs (MPA; 0.47 and QC; 0.36). Moreover, the apoptosis index (0.91) was significantly higher in LPNs combination (MPA-LPN + QC-LPN) compared to the combination of free drugs (free MPA + free QC, apoptosis index 0.56). These results were consistent with the results obtained in the MTT assay.

Inosine-5′-monophosphate dehydrogenase (IMPDH) activity

Inosine-5′-monophosphate dehydrogenase (IMPDH) catalyzed step referred to the rate-limiting step in the synthesis of DNA and RNA precursor (guanosine triphosphate) by converting inosine monophosphate (IMP) to xanthosine monophosphate (XMP) using NAD^+ as a cofactor. IMPDH has species-specific properties and inhibitor sensitivities; hence, this enzyme could be a target for the treatment of various diseases like cancer, graft rejection, virus, and bacterial infections. Thus, for new drug design and screening of disease, IMPDH measurement may serve as a useful tool. The previous reports showed that expression of IMPDH is more in tumor cells as compared to the normal ones; hence it may be a potential target for the treatment of cancer.[7,13] Here we have studied the effect of free MPA and MPA-LPN on IMPDH activity in MCF-7 cells. From Figure 6, *A*, it is clear that the activity of the IMPDH enzyme was higher in control than that of free MPA and MPA-LPNs due to their enzyme inhibitory action which was 2.11 and 5.85 folds, respectively. Here, significantly higher enzyme inhibition was observed in MPA-LPN than free MPA.

Pharmacokinetics

Various pharmacokinetic factors after *i.p.* administration of free MPA, free MPA + free QC, MPA-LPN, and MPA-LPN + QC-LPN are summarized in Table 5. Compared to free MPA, the $AUC_{(0-\infty)}$ and $T_{1/2}$ values of MPA in the MPA-LPN group were found to be 2.37 and 1.84 fold higher, respectively. Similarly, combination therapy of MPA-LPN + QC-LPN demonstrated 1.31 and 1.18 fold higher $AUC_{(0-\infty)}$ and $T_{1/2}$ values, respectively, as compared to only MPA-LPN for their pharmacokinetic profiles after *i.p.* administration (Figure 6, *B*). The overall $AUC_{(0-\infty)}$ and $T_{1/2}$ values of MPA were increased 3.11 and 2.17 folds, respectively in combination therapy of nanoparticle compared to fee MPA.

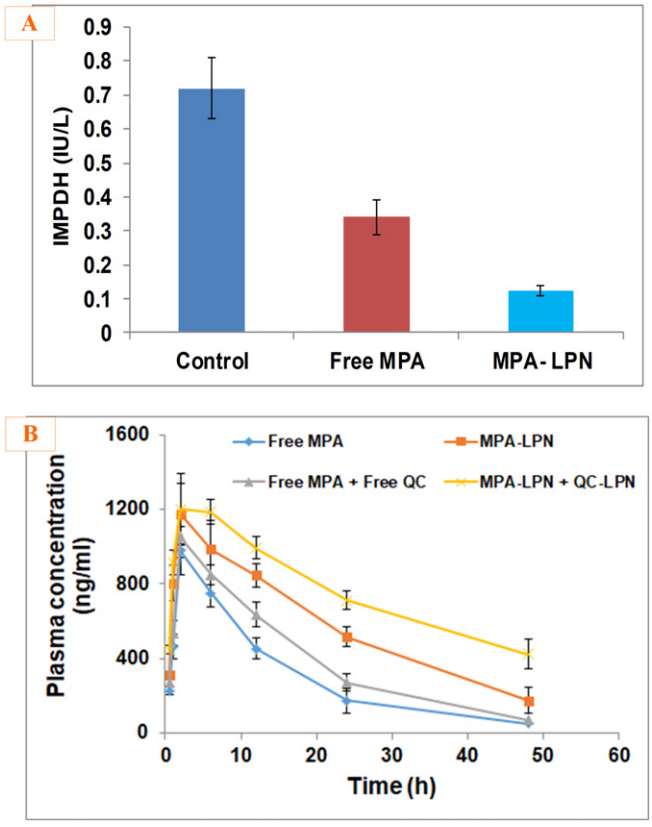

Figure 6. **(A)** Effect of free MPA and MPA-LPN on inosine-5′-monophosphate dehydrogenase activity in MCF-7 cell lines. **(B)** Plasma concentration–time profiles of free MPA, MPA-LPN, free MPA+ free QC, and MPA-LPN + QC-LPN following the i.p. administration in rats.

In vivo antitumor efficacy and tissue distribution

In vivo pharmacodynamic efficacy of developed LPNs was tested in DMBA induced breast cancer tumor model. Treatment with combination therapy of MPA and QC loaded LPNs has demonstrated a significant reduction in the tumor burden in comparison to free MPA, free QC, and their combination (free MPA + free QC). Figure 7, *A* showed the antitumor activity and tumor burden of free MPA, free QC, free MPA + free QC, MPA-LPN, QC-LPN, and combination therapy of MPA-LPN + QC-LPN following the *i.p.* administration. Combination therapy of MPA and QC loaded LPN treated animals demonstrated significant suppression of tumor growth ($P < 0.001$) as compared to other groups (Figure 7, *C*). In combination therapy of MPA and QC loaded LPN, the size of the tumor (in percent) was found to be 32.5%, as compared to the control group where tumor size was 154.29% after 30 days of treatment (Figure 7, *B*). Furthermore, combination therapy of MPA and QC loaded LPN showed enhanced survival time of tumor-bearing rats in LPN treated groups as compared to DMBA

Table 5
Pharmacokinetic parameters of LPN upon i.p. administration in rats.

Parameters	MPA	MPA-LPN	MPA + QC	MPA LPN + QC LPN
AUC (ng/mL·h)	11,533.79 ± 969.5	27,395.9 ± 1467.4	15,478.21 ± 1004.5	35,898.79 ± 2069.5
C_{max} (ng/mL·h)	979.3 ± 89.5	1175.34 ± 123	1054.38 ± 98.5	1204.39 ± 121
$T_{1/2}$ (h)	13.07 ± 0.98	24.12 ± 1.98	16.79 ± 1.1	28.41 ± 2.7
MRT (h)	18.16 ± 1.4	34.01 ± 3.5	22.84 ± 1.6	46 ± 2.8

AUC, area under curve; C_{max}, maximum drug concentration; $T_{1/2}$, time to reach half of maximum plasma concentration; MRT, mean retention time.

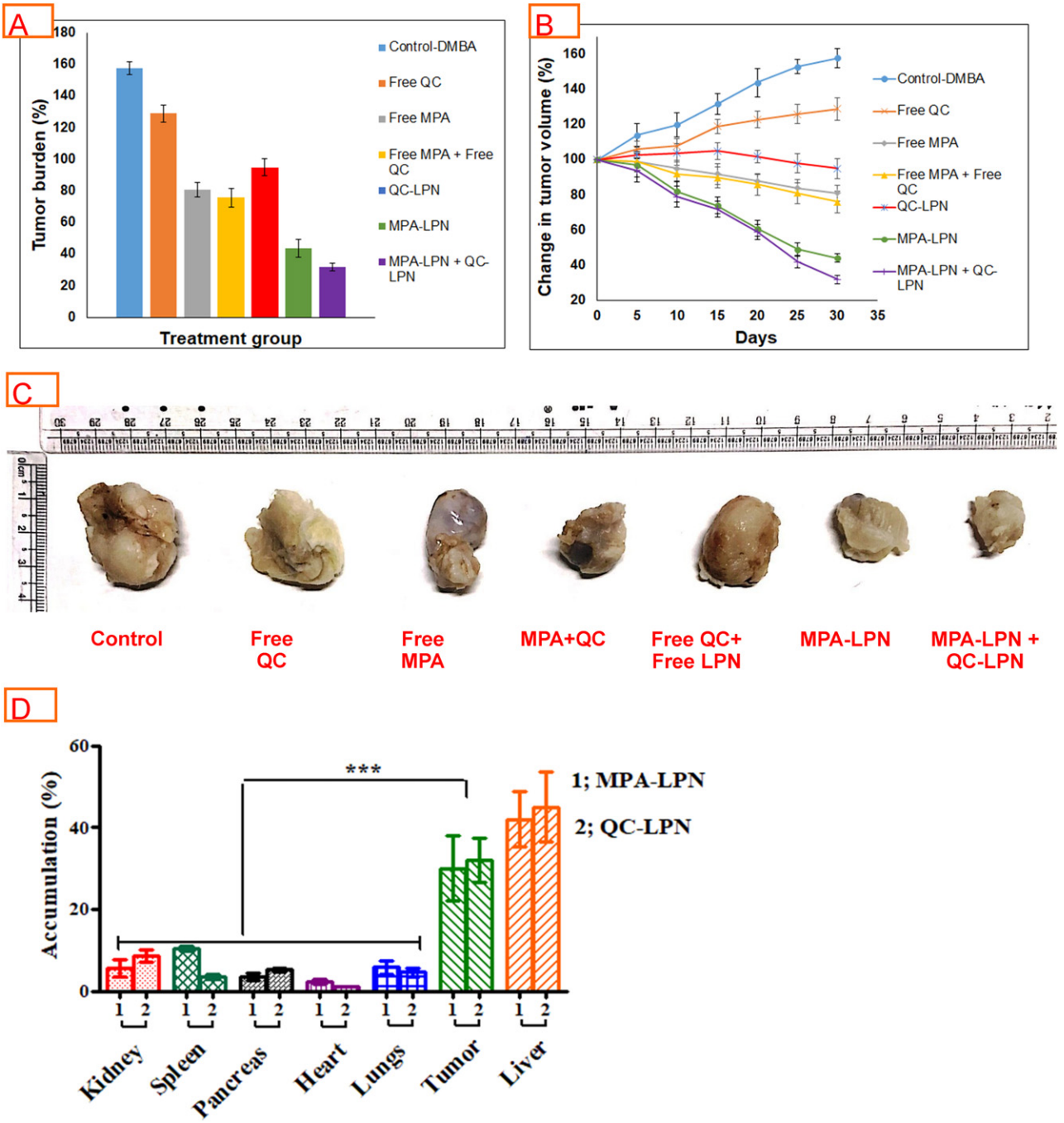

Figure 7. **(A)** Comparison of % change in tumor volume treated with different formulation and their combination. **(B)** % tumor burden in animals treated with different formulations. **(C)** Representative photographs of excised tumors from different treatment groups. **(D)** Drug distribution profile of MPA and QC in the various organ of SD rat.

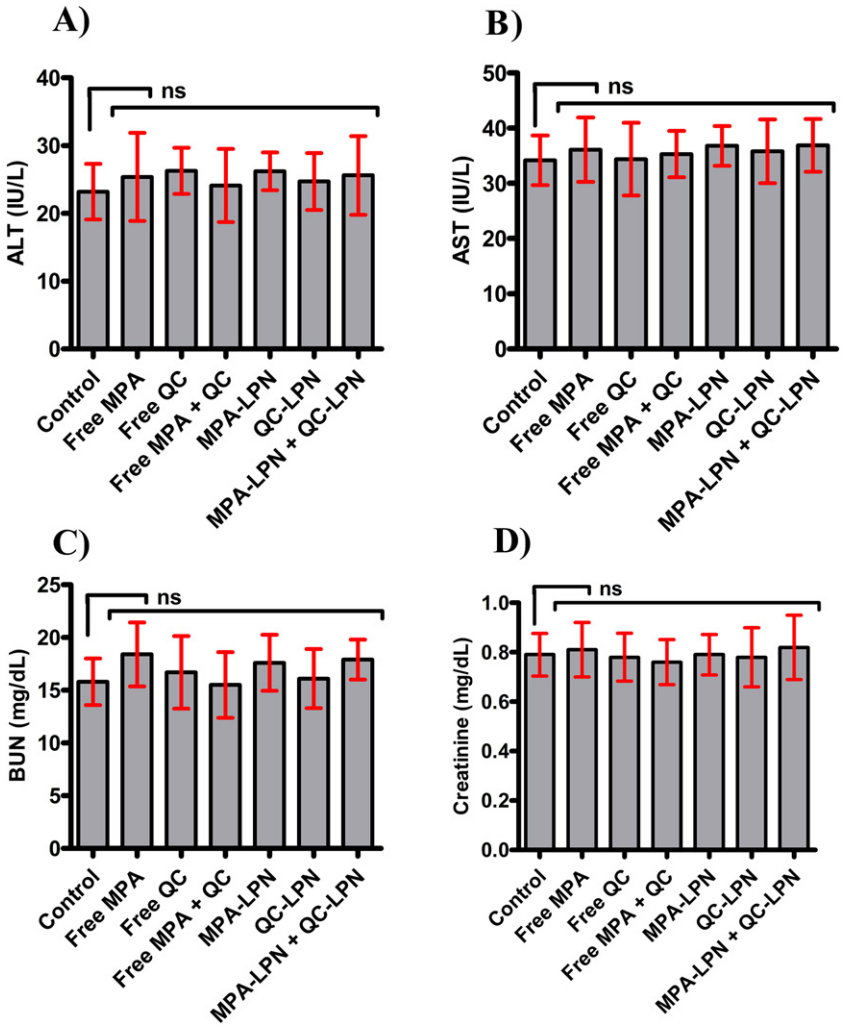

Figure 8. Toxicity profile of free MPA, free QC, free MPA + free QC, MPA-LPN, QC-LPN, and MPA-LPN + QC-LPN.

control and other groups suggestive of lower toxicity and higher safety of the developed combinatory strategy. Moreover, the accumulation of the MPA and QC was also determined in different organs and compared to the accumulation of the drug in the targeted tumor tissue. Figure 7, *D* revealed that MPA and QC concentrations were more in the tumor compared to the kidneys, spleen, pancreas, lungs, and heart. However, the maximum accumulated concentration of MPA and QC was found in the liver**.**

In vivo toxicity of profile

The hepatotoxicity is one of the most associated side effects of conventional treatment. The various biochemical markers were determined for the toxicity evaluation of developed nanoparticles.[37,43,45] From Figure 8, it is clear that no significant differences were observed in the plasma concentrations of ALT, AST, creatinine, and BUN. These studies revealed the more clinical safety of prepared LPNs. The concentration ranges of several hepatotoxicity biomarkers (ALT and AST) were insignificant as compared to control, confirming minimal toxicity of nanoformulations (Figure 8, *A* and *B*). Minimal hepatic cell damage occurs due to the neutral effect of the LPNs. Furthermore, no nephrotoxicity was observed due to LPNs as insignificant changes in the plasma concentration of BUN and creatinine occurred (Figure 8, *C* and *D*). The toxicity profile of the developed formulations suggested high clinical safety and suitability.

Discussion

The present investigation reports preparation, optimization, and characterization of MPA and QC loaded LPNs, individually. The primary characterization of prepared nanoparticles was carried out by dynamic light scattering (DLS) and Zeta potential analysis. Transmission electron microscope (TEM) was used to further confirmation of morphology of synthesized nanoparticles. DLS generally measures the bigger size of nanoparticle than their actual diameters because the DLS measures the

hydrodynamic diameter through the scattering of light from the hydrated nanoparticle, while TEM measures the size of nanoparticle through diffraction technique (Table 1).[46,47] Moreover, the results obtained from TEM were found to be in good correlation with the results obtained from zeta sizer.[48,49] FTIR analysis of free drugs and their nanoparticles revealed the intact chemical properties of each component (Figure 2, *A*). The XRD diffractogram of drug-loaded LPN showed that the intensity of the characteristic peak of free drug molecules decreased or was completely concealed confirming their entrapment in the polymeric core of the LPN (Figure 2, *B*).[50]

In encapsulation studies, it is evidenced from Figure 3, *A* EE of QC was better as compared to MPA; however, the nature of both drugs is hydrophobic. The developed LPNs were then analyzed for *in vitro* hydrolysis to evaluate the release behavior of MPA and QC at pH 7.4. Thus, the drug release pattern for both the drugs demonstrated a slow, uniform, controlled and biphasic release profile. Initially, more release of the drug may be due to the quick release of adsorbed and diffused drug from the surface of LPNs.[51,52] From Figure 3, *B*, it is clear that the releasing rate of QC-LPN was slower than MPA-LPN. It may be due to QC having less aqueous solubility in pH -7.4 phosphate buffer compared to MPA-LPN. In cryoprotectants experiments, mannitol was employed as the optimized one owing to the formation of the stable network around the LPN leading to minimal changes in the critical quality attributes of LPNs. In the stability studies, there was no significant difference observed in the size and shape of prepared nanoparticles after 6 months of testing period.[53]

The cell cytotoxicity assay revealed significantly higher cell cytotoxicity of LPNs against MCF-7 cells as compared to free drugs (MPA and QC) and their combination (free MPA + free QC) in both concentration and time-dependent manner (Figure 4, *C*). Higher cell cytotoxicity of LPNs might be due to more drug uptake through additional endocytosis pathway and better stability of MPA in the nanoformulation.[24,48,53] While the free drug (free MPA and free QC) and their combination (free MPA and free QC) showed poor cell cytotoxicity which might be due to higher P-gp mediated efflux bypassing endocytosis and less cell uptake *via* saturable hNTs (MPA) and OATP1B3 (for QC) transporter.[50] It is clear from Figure 4 that C6 loaded LPNs were efficiently internalized by the MCF-7 cells within 2 h of incubation as compared to free C-6 suggesting the efficient internalization of LPNs by MCF-7 cells. As demonstrated from Figure 5, apoptosis analysis the combination of LPN (MPA-LPN + QC-LPN) shown more red fluorescence and apoptosis index compared to alone MPA-LPN, QC-LPN, free MPA, free QC and combination of free drug. It may due to more retention within the cell and higher cellular uptake (through clathrin-mediated) of nanoparticles.[54,55] In another study IMPDH enzyme inhibition by MPA-LPN revealed the advanced efficacy of formulation over the free drug that might be due to higher internalization of nanoparticles compared to the free drugs.[24,25]

The *in vivo* pharmacokinetic profile of free MPA, free MPA + free QC, MPA-LPN and combination of MPA-LPN + QC-LPN was evaluated. These studies shown that the $AUC_{(0-\infty)}$ and $T_{1/2}$ values were found more in case of nanoparticles and maximum in the combination of MPA-LPN + QC-LPN. This increment of AUC and $T_{1/2}$ values might be due to two reasons; first sustained release of drug from nanoparticles and second the increased blood residence time of MPA due to inhibition of its metabolism through cytochrome P450 enzyme by QC. Cytochrome P450 is the main enzyme that metabolized the MPA into inactive MPAG and AcMPAG and its inhibition led to reduced susceptibility towards the renal clearance or filtration.[56] Treatment with LPN in DMBA induced breast tumor-bearing rats exhibited a significant reduction in the tumor burden compared to free MPA, free QC, and their combination, which might be due to the sustained release of drugs and significantly higher bioavailability.[23–25] Higher efficacy may also due to the increased half-life of MPA by inhibition of MPA metabolism through QC. The increased therapeutic efficacy of LPN could be attributed to sustained pharmacokinetic patterns responsible for longer availability of MPA and QC in the blood compartment and by the virtue of enhanced permeation and retention (EPR) effect[50,51,57] Enhanced efficacy in the case of developed LPN could be attributed to the higher tumor accumulation due to higher uptake by both clathrin and caveolae-mediated uptake.[58,59] Thus, the EPR effect along with the enhanced selective tumor cellular uptake will ensure the distribution of drug-loaded LPN in the tumor vicinity, which, in turn, is expected to enhance the therapeutic efficacy of the loaded drug with reduced drug-induced toxicity.[48,52]

In the present report, combination therapy of (MPA-LPN + QC-LPN) based co-formulation was developed to overcome the associated hurdles with the individual drugs and the combination to improve the therapeutic efficacy. The said combination in LPN posed higher cell cytotoxicity and antitumor tumor efficacy in contrast to the free drug combination. Moreover, co-administration of antioxidant supports in alleviating the free radical-induced oxidative stress generated during the course of chronic therapy of MPA. The results demonstrated that the developed LPNs are stable against conversion into free drugs and are safe for the i.p. administration of both MPA and QC. In nutshell, the developed formulation strategy poses great potential for synchronized delivery of co-administered drugs leading to the increased bioavailability, therapeutic efficacy, and safety profile of the combination.

References

1. Pandey A, Soccol CR, Mitchell D. New developments in solid state fermentation: I-bioprocesses and products. *Process Biochem* 2000;**35**:1153-69.
2. Lafont P, Debeaupuis JP, Gaillardin M, Payen J. Production of mycophenolic acid by *Penicillium roqueforti* strains. *Appl Environ Microbiol* 1979;**37**:365-8.
3. Kitchin JES, Pomeranz MK, Pak G, Washenik K, Shupack JL. Rediscovering mycophenolic acid: a review of its mechanism, side effects, and potential uses. *J Am Acad Dermatol* 1997;**37**:445-9.
4. Patro JP, Priyadarsini P. Mycophenolic acid : a drug with a potential beyond renal transplantation. *Int J Res Med Sci* 2016;**4**:3666-9.
5. Patel G, Biswas K, Patil MD, Chisti Y, Banerjee UC. Bioreactor studies of production of mycophenolic acid by *Penicillium brevicompactum*. *Biochem Eng J* 2018;**140**:77-84 Available from: https://doi.org/10.1016/j.bej.2018.09.007.
6. Patel G, Patil MD, Soni S, Chisti Y, Banerjee UC. Production of mycophenolic acid by *Penicillium brevicompactum* using solid state

fermentation. *Appl Biochem Biotechnol* 2017;**182**:97-109 Available from: http://link.springer.com/10.1007/s12010-016-2313-3.
7. Majd N, Sumita K, Yoshino H, Chen D, Terakawa J, Daikoku T, et al. A review of the potential utility of mycophenolate mofetil as a cancer therapeutic. *J Cancer Res* 2014;**2014**:1-12 Available from: http://www.hindawi.com/archive/2014/423401/.
8. Zheng ZH, Yang Y, Lu XH, Zhang H, Shui XX, Liu C, et al. Mycophenolic acid induces adipocyte-like differentiation and reversal of malignancy of breast cancer cells partly through PPARγ. *Eur J Pharmacol* 2011;**658**:1-8.
9. Dun B, Xu H, Sharma A, Liu H, Yu H, Yi B, et al. Delineation of biological and molecular mechanisms underlying the diverse anticancer activities of mycophenolic acid. *Int J Clin Exp Pathol* 2013;**6**:2880-6.
10. Thakur NS, Patel G, Kushwah V, Jain S, Banerjee UC. Self-assembled gold nanoparticle–lipid nanocomposites for on-demand delivery, tumor accumulation, and combined photothermal–photodynamic therapy. *ACS Appl Bio Mater* 2019;**2** 349–36.
11. Eugui EM, Almquist SJ, Muller CD, Allison AC. Lymphocyte-selective cytostatic and immunosuppressive effects of mycophenolic acid *in vitro*: role of deoxyguanosine nucleotide depletion. *Scand J Immunol* 1991;**33**:161-73.
12. Allison AC, Eugui EM. Mycophenolate mofetil and its mechanisms of action. *Immunopharmacology* 2000;**47**:85-118.
13. Fellenberg J, Kunz P, Sähr H, Depeweg D. Overexpression of inosine 5′-monophosphate dehydrogenase type II mediates chemoresistance to human osteosarcoma cells. *PLoS ONE* 2010;**5**12179.
14. Sweeney MJ, Gerzon K, Harris PN, Holmes RE, Poore GA, Robert H. Experimental antitumor activity and preclinical toxicology of mycophenolic acid experimental antitumor activity and preclinical toxicology of mycophenolic acid. *Cancer Res* 1972;**32**:1795-802.
15. Végso G, Sebestyén A, Paku S, Barna G, Hajdu M, Tóth M, et al. Antiproliferative and apoptotic effects of mycophenolic acid in human B-cell non-Hodgkin lymphomas. *Leuk Res* 2007;**31**:1003-8.
16. Takebe N. IMP dehydrogenase inhibitor mycophenolate mofetil induces caspase-dependent apoptosis and cell cycle inhibition in multiple myeloma cells. *Mol Cancer Ther* 2006;**5**:457-66.
17. Dun B, Sharma A, Teng Y, Liu H, Purohit S, Xu H, et al. Mycophenolic acid inhibits migration and invasion of gastric cancer cells via multiple molecular pathways. *PLoS ONE* 2013;**8**:1-12.
18. Shaw LM, Korecka M, DeNofrio D, Brayman KL. Pharmacokinetic, pharmacodynamic, and outcome investigations as the basis for mycophenolic acid therapeutic drug monitoring in renal and heart transplant patients. *Clin Biochem* 2001;**34**:17-22.
19. Spencer CM, Goa KL, Tacrolimus Gillis JC. An update of its pharmacology and clinical efficacy in the management of organ transplantation. *Drugs* 1997;**54**:925-75.
20. Look M, Stern E, Wang QA, DiPlacido LD, Kashgarian M, Craft J, et al. Nanogel-based delivery of mycophenolic acid ameliorates systemic lupus erythematosus in mice. *J Clin Inves* 2013;**123**:1741-9.
21. Shirali AC, Look M, Du W, Kassis E, Stout-Delgado HW, Fahmy TM, et al. Nanoparticle delivery of mycophenolic acid upregulates PD-L1 on dendritic cells to prolong murine allograft survival. *Am J Transplant* 2011;**11**:2582-92.
22. Hwang J, Lee E, Kim J, Seo Y, Lee KH, Hong JW, et al. Effective delivery of immunosuppressive drug molecules by silica coated iron oxide nanoparticles. *Colloids Surf B Biointerfaces* 2016;**142**:290-6 Available from: https://doi.org/10.1016/j.colsurfb.2016.01.040.
23. Mukherjee A, Waters AK, Kalyan P, Achrol AS, Kesari S, Yenugonda VM. Lipid-polymer hybrid nanoparticles as a nextgeneration drug delivery platform: state of the art, emerging technologies, and perspectives. *Int J Nanomedicine* 2019;**14**:1937-52.
24. Duan R, Li C, Wang F, Yangi JC. Polymer–lipid hybrid nanoparticles-based paclitaxel and etoposide combinations for the synergistic anticancer efficacy in osteosarcoma. *Colloids Surf B Biointerfaces* 2017;**159**:880-7 Available from: https://doi.org/10.1016/j.colsurfb.2017.08.042.
25. Zhang LJ, Wu B, Zhou W, Wang CX, Wang Q, Yu H, et al. Two-component reduction-sensitive lipid-polymer hybrid nanoparticles for triggered drug release and enhanced: *in vitro* and *in vivo* anti-tumor efficacy. *Biomater Sci* 2017;**5**:98-110.
26. Zhu X, Zeng X, Zhang X, Cao W, Chang D, He S, et al. The effects of quercetin-loaded PLGA-TPGS nanoparticles on ultraviolet B-induced skin damages *in vivo*. *Nanomedicine Nanotechnology, Biol Med* 2016;**12**:623-32 Available from: https://doi.org/10.1016/j.nano.2015.10.016.
27. Kashyap D, Mittal S, Sak K, Singhal P, Tuli HS. Molecular mechanisms of action of quercetin in cancer: recent advances. *Tumor Biol* 2016;**37**:12927-39 Available from: https://doi.org/10.1007/s13277-016-5184-x.
28. Lautraite S. Flavonoids inhibit genetic toxicity produced by carcinogens in cells expressing CYP1A2 and CYP1A1. *Mutagenesis* 2002;**17**:45-53.
29. Tetsuka K, Gerst N, Tamura K, Masters JN. Glucuronidation and subsequent biliary excretion of mycophenolic acid in rat sandwich-cultured hepatocytes. *Drug Metab Pharmacokinet* 2013;**29**:129-34.
30. Shin J, Yin Y, Kim DK, Kim DW, Hong J. Foxp3 plasmid-encapsulated PLGA nanoparticles attenuate pain behavior in rats with spinal nerve ligation. *Nanomedicine Nanotechnology, Biol Med* 2019;**18**:90-100 Available from:https://doi.org/10.1016/j.nano.2019.02.023.
31. Chan JM, Zhang L, Yuet KP, Liao G, Rhee JW, Langer R, et al. PLGA-lecithin-PEG core-shell nanoparticles for controlled drug delivery. *Biomaterials* 2009;**30**:1627-34.
32. Ra L. X-ray diffraction. *J Chem Educ* 1958;**35**:80-3.
33. Kumbhar DD, Pokharkar VB. Physicochemical investigations on an engineered lipid-polymer hybrid nanoparticle containing a model hydrophilic active, zidovudine. *Colloids Surf A Physicochem Eng Asp* 2013;**436**:714-72.
34. Mandal B, Mittal NK, Balabathula P, Thoma LA, Wood GC. Development and *in vitro* evaluation of core-shell type lipid-polymer hybrid nanoparticles for the delivery of erlotinib in non-small cell lung cancer. *Eur J Pharm Sci* 2016;**81**:162-71.
35. Gao J, Xia Y, Chen H, Yu Y, Song J, Li W, et al. Polymer–lipid hybrid nanoparticles conjugated with anti-EGF receptor antibody for targeted drug delivery to hepatocellular carcinoma. *Nanomedicine* 2014;**9**:279-93.
36. Durán V, Yasar H, Becker J, Thiyagarajan D, Loretz B, et al. Preferential uptake of chitosan-coated PLGA nanoparticles by primary human antigen presenting cells. *Nanomedicine Nanotechnology, Biol Med* 2019;**21**:102073 Available from:https://doi.org/10.1016/j.nano.2019.102073.
37. Jain AK, Thanki K, Jain S. Co-encapsulation of tamoxifen and quercetin in polymeric nanoparticles: implications on oral bioavailability, antitumor efficacy, and drug-induced toxicity. *Mol Pharm* 2013;**10**:3459-74.
38. Pissinate K, Rostirolla DC, Pinheiro LM, Suryadevara P, Yogeeswari P, Sriram D, et al. Synthesis and evaluation of thiazolyl-1h-benzo[d] imidazole inhibitors of *Mycobacterium tuberculosis* inosine monophosphate dehydrogenase. *J Braz Chem Soc* 2015;**26**:1357-66.
39. Jeon SG, Cha MY, Kim J, Hwang TW, Kim KA, Kim TH, et al. Vitamin D-binding protein-loaded PLGA nanoparticles suppress Alzheimer's disease-related pathology in 5XFAD mice. *Nanomedicine Nanotechnology, Biol Med* 2019;**17**:297-307 Available from:https://doi.org/10.1016/j.nano.2019.02.004.
40. Shah P, Jimeno A, Viqueira BR, Zhang X, Cusatis G, Chong C, et al. *In vivo* testing of mycophenolic acid (MPA) in primary pancreatic cancer (PaCa) xenografts. *Journal of J Cancer Res* 2007;**67**.
41. Patel G, Patil MD, Soni S, Khobragade TP, Chisti Y, Banerjee UC. Production of mycophenolic acid by *Penicillium brevicompactum* — a comparison of two methods of optimization. *Biotechnol Reports* 2016;**11**:77-85.
42. Dastidar DG, Das A, Datta S, Ghosh Suvranil P, Pal M, Thakur NS, et al. Paclitaxel-encapsulated core-shell nanoparticle of cetyl alcohol for active targeted delivery through oral route. *Nanomedicine* 2019;**14**:2121-50.

43. Thakur NS, Patel G, Kushwah V, Jain S, Banerjee UC. Facile development of biodegradable polymer-based nanotheranostics: hydrophobic photosensitizers delivery, fluorescence imaging and photodynamic therapy. *J Photochem Photobiol B, Biol* 2019;**193**:39-50.
44. Cano A, Ettcheto M, Espina M, Auladell C, Calpena AC, Folch J, et al. Epigallocatechin-3-gallate loaded PEGylated-PLGA nanoparticles : a new anti-seizure strategy for temporal lobe epilepsy. *Nanomedicine Nanotechnology, Biol Med* 2018;**14**:1073-85 Available from: https://doi.org/10.1016/j.nano.2018.01.019.
45. Gao Y, Yang R, Zhang Z, Chen L, Sun Z, Li Y. Solid lipid nanoparticles reduce systemic toxicity of docetaxel: performance and mechanism in animal. *Nanotoxicology* 2011;**5**:636-49.
46. Bhaumik J, Thakur NS, Aili PK, Ghanghoriya A, Mittal AK, Banerjee Uttam C. Bioinspired nanotheranostic agents: synthesis, surface functionalization, and antioxidant potentia. *ACS Biomater Sci Eng* 2015;**1**:382-92.
47. Thakur NS, Bhaumik J, Kirar S, Banerjee UC. Development of gold-based phototheranostic nanoagents through a bioinspired route and their applications in photodynamic therapy. *ACS Sustain Chem Eng* 2017;**5**:7950-60.
48. Su X, Wang Y, Wang W, Sun K, Chen L. Phospholipid encapsulated AuNR@Ag/au nanosphere SERS tags with environmental stimulus responsive signal property. *ACS Appl Mater Interfaces* 2016;**8**:10201-11.
49. Peng H, Xiong H, Li J, Chen L, Zhao Q. Methoxy poly(ethylene glycol)-grafted-chitosan based microcapsules: synthesis, characterization and properties as a potential hydrophilic wall material for stabilization and controlled release of algal oil. *J Food Eng* 2010;**101**:113-9.
50. Mu Q, Jiang G, Chen L, Zhou H, Fourches D, Tropsha A, et al. Chemical basis of interactions between engineered nanoparticles and biological systems. *Chem Rev* 2014;**114**:7740-81.
51. Mei R, Wang Y, Liu W, Chen L. Lipid bilayer-enabled synthesis of waxberry-like core-fluidic satellite nanoparticles: toward ultrasensitive surface-enhanced raman scattering tags for bioimaging. *ACS Appl Mater Interfaces* 2018;**10**:23605-16.
52. Song X, Li J, Wang J, Chen L. Quercetin molecularly imprinted polymers: preparation, recognition characteristics and properties as sorbent for solid-phase extraction. *Talanta* 2009;**80**:694-702.
53. Ren T, Wang Q, Xu Y, Cong L, Gou J, Tao X, et al. Enhanced oral absorption and anticancer efficacy of cabazitaxel by overcoming intestinal mucus and epithelium barriers using surface polyethylene oxide (PEO) decorated positively charged polymer-lipid hybrid nanoparticles. *J Control Release* 2018;**269**:423-38.
54. Huang H, Dong Y, Zhang Y, Ru D, Wu Z, Zhang J, et al. GSH-sensitive Pt(IV) prodrug-loaded phase-transitional nanoparticles with a hybrid lipid-polymer shell for precise theranostics against ovarian cancer. *Theranostics* 2019;**9**:1047-65.
55. Muniswamy VJ, Raval N, Gondaliya P, Tambe V, Kalia K, Tekade RK. 'Dendrimer-Cationized-albumin' encrusted polymeric nanoparticle improves BBB penetration and anticancer activity of doxorubicin. *Int J Pharm* 2019;**555**:77-99.
56. Kontermann RE. Strategies for extended serum half-life of protein therapeutics. *Curr Opin Biotechnol* 2011;**22**:868-76.
57. Kirar S, Thakur NS, Laha JK, Banerjee UC. Porphyrin functionalized gelatin nanoparticle-based biodegradable phototheranostics: potential tools for antimicrobial photodynamic therapy. *ACS Appl Bio Mater* 2019;**2**:4202-12.
58. Simons M. An inside view: vegf receptor trafficking and signaling. *Phys Ther* 2012;**27**:213-22.
59. Desai N. Nab technology: a drug delivery platform utilising endothelial gp60 receptor-based transport and tumour-derived sparc for targeting. *Drug delivery report* 2007:37-41.